Ca^{2+} Dynamics in a Population of Smooth Muscle Cells: Modeling the Recruitment and Synchronization

Michèle Koenigsberger,* Roger Sauser,* Mathieu Lamboley,* Jean-Louis Bény,† and Jean-Jacques Meister*
*Laboratory of Cell Biophysics, Swiss Federal Institute of Technology, Lausanne, Switzerland; and †Department of Zoology and Animal Biology, University of Geneva, Geneva, Switzerland

ABSTRACT Many experimental studies have shown that arterial smooth muscle cells respond with cytosolic calcium rises to vasoconstrictor stimulation. A low vasoconstrictor concentration gives rise to asynchronous spikes in the calcium concentration in a few cells (asynchronous flashing). With a greater vasoconstrictor concentration, the number of smooth muscle cells responding in this way increases (recruitment) and calcium oscillations may appear. These oscillations may eventually synchronize and generate arterial contraction and vasomotion. We show that these phenomena of recruitment and synchronization naturally emerge from a model of a population of smooth muscle cells coupled through their gap junctions. The effects of electrical, calcium, and inositol 1,4,5-trisphosphate coupling are studied. A weak calcium coupling is crucial to obtain a synchronization of calcium oscillations and the minimal required calcium permeability is deduced. Moreover, we note that an electrical coupling can generate oscillations, but also has a desynchronizing effect. Inositol 1,4,5-trisphosphate diffusion does not play an important role to achieve synchronization. Our model is validated by published in vitro experiments obtained on rat mesenteric arterial segments.

INTRODUCTION

The regulation of hemodynamics by variations of the arterial diameter results from the contraction of smooth muscle cells (SMCs) present in the muscular arterial wall. Many experimental studies have shown that the contraction of arteries and arterioles is due to an increase in the mean cytosolic calcium concentration measured on segments of the arterial wall (Meininger et al., 1991; Wagner et al., 1996; Yip and Marsh, 1996; Dora et al., 1997). Calcium increases result from the release of vasoconstrictors present in the arterial system. Recently, it has been possible to observe that the average vessel calcium concentration is not representative of the calcium dynamics within individual SMCs in the vessel wall (Ruehlmann et al., 2000; Zang et al., 2001; Mauban et al., 2001; Peng et al., 2001; Sell et al., 2002; Lamboley et al., 2003): phenomena such as flashing, recruitment, and synchronization have been reported. These studies make use of vasoconstrictors like vasopressin, norepinephrine (NE), phenylephrine (PE), or potassium chloride (KCl). At low vasoconstrictor concentrations, there are only asynchronous calcium rises (asynchronous flashing) in few SMCs and no vessel contraction. Above a certain vasoconstrictor concentration, all SMCs are recruited (all cells are flashing). A simultaneous recruitment leads to a local vessel contraction. Depending on the vessel type and the nature of the vasoconstrictor, different behaviors have been observed. On rat mesenteric arteries, KCl induces one large synchronous calcium increase followed by small asynchronous oscillations (Lamboley et al., 2003). The same arteries stimulated by NE (Peng et al., 2001; Sell et al., 2002) and PE (Mauban et al., 2001; Lamboley et al., 2003) present synchronous calcium oscillations, leading to a cyclic variation of vascular basal tone with time (vasomotion). On the other hand, Ruehlmann et al. (2000) have observed asynchronous oscillations on the rabbit inferior vena cava with PE. Raising the vasoconstrictor concentration increases the oscillations frequency (Ruehlmann et al., 2000; Lamboley et al., 2003) and very high vasoconstrictor concentrations lead to an elevated mean calcium level and to a tonic contraction (Lamboley et al., 2003).

To the best of our knowledge, no existing theoretical model describes the flashing and recruitment of a population of SMCs, and the synchronization of their calcium oscillations. Several biophysical models propose mechanisms for the origin and dynamics of arterial or arteriolar vasomotion, without taking into account intercellular communication. According to Ursino et al. (1992) and Achakri et al. (1994), vasomotion originates from the interaction between external loads (like pressure and flow), the mechanical properties of an artery, and the mechanisms controlling vascular tone. However, the experiments of Lamboley et al. (2003), performed on rat mesenteric arterial strips without external loads, exhibit synchronous calcium oscillations leading to vasomotion. To understand the origin of arterial vasomotion, another possible approach is to describe the calcium dynamics of a single SMC (Gonzalez-Fernandez and Ermentrout, 1994; Parthimos et al., 1999).

In this article, we propose a model describing a population of coupled SMCs. As contraction and vasomotion have also been observed in absence of an intact endothelium (Haddock

Submitted December 3, 2003, and accepted for publication March 16, 2004.

Address reprint requests to Michèle Koenigsberger, Laboratory of Cell Biophysics, Swiss Federal Institute of Technology, CH-1015 Lausanne, Switzerland. Tel.: 4-121-693-8347; Fax: 4-121-693-8305; E-mail: michele.koenigsberger@epfl.ch.

0006-3495/04/07/92/13 $2.00

doi: 10.1529/biophysj.103.037853

et al., 2002; Lamboley et al., 2003), endothelial cells are not included in the model. To describe the calcium dynamics in a single SMC, we extend the model of Parthimos et al. (1999), which is to the best of our knowledge the most advanced model of SMCs. It reproduces well experimental findings (arterial vasomotion) and is able to simulate various pharmacological interventions on SMCs. Gap junctions have been shown to play a role in the intercellular communication between SMCs (Christ et al., 1992, 1996). M. Lamboley, P. Pittet, M. Koenigsberger, R. Sauser, J.-L. Bény, and J.-J. Meister (unpublished results) have observed that adding a gap junction inhibitor to a population of synchronized SMCs leads to complete loss of synchrony, although the cells continue oscillating. Therefore gap junctions are assumed to be necessary for synchronization.

As gap junctions are only poorly selective (Christ et al., 1996), one can consider a priori three different possibilities to synchronize calcium oscillations in SMCs: through electrical coupling, inositol 1,4,5-trisphosphate (IP_3) diffusion, and, obviously, calcium diffusion. An electrical coupling is a reasonable possibility, because SMCs are excitable cells and the membrane potential oscillates during contraction and vasomotion (Shimamura et al., 1999; Oishi et al., 2002). Peng et al. (2001) suggest that initially asynchronous elevated calcium levels in individual SMCs activate a depolarizing current that spreads to all SMCs and could then lead to a synchronous calcium influx through voltage-operated calcium channels (VOCCs). IP_3 diffusion could also be responsible for synchronization of calcium oscillations, as IP_3 diffuses faster than calcium. However, under constant drug stimulation, the IP_3 level is assumed not to vary in an oscillating cell (Wakui et al., 1989; Savineau and Marthan, 2000), unless the cell presents a phospholipase C-δ (PLC-δ), which is the case of many types of SMCs (LaBelle and Polyak, 1996; Lymn and Hughes, 2000). In fact this isoform of PLC is activated by low concentrations of calcium (Rebecchi and Pentyala, 2000), and so calcium oscillations can give rise to IP_3 oscillations that in turn could synchronize the calcium oscillations.

The aim of this study is to gain insights into the emergent properties of a population of coupled SMCs stimulated by receptor-ligand agonists and KCl. In particular, we model the flashing, recruitment, and synchronization of SMCs and determine what coupling mechanism is required to synchronize calcium oscillations. The different behaviors elicited by the coupling of SMCs are studied and a value for the gap junctional calcium permeability is deduced. The model is then compared to the in vitro results of Lamboley et al. (2003) obtained on rat mesenteric arterial segments.

MATHEMATICAL MODEL

Single-cell model

We extend the model of Parthimos et al. (1999) to describe the calcium dynamics of a single SMC *i*. In the approach of Parthimos et al. (1999), the calcium transients and oscillations are generated by the nonlinear interaction of two oscillators: an intracellular oscillator and a membrane oscillator (Griffith and Edwards, 1994). The model has four variables: the calcium concentration in the cytosol c_i, the calcium concentration in the sarcoplasmic reticulum (SR) s_i, the cell membrane potential v_i, and the open state probability w_i of calcium-activated potassium channels. The variables c_i and s_i set up the intracellular oscillator, and v_i and w_i the membrane oscillator (Parthimos et al., 1999):

$$\frac{dc_i}{dt} = J_{IP3_i} - J_{VOCC_i} + J_{Na/Ca_i} - J_{SRuptake_i} + J_{CICR_i} - J_{extrusion_i} + J_{leak_i}, \quad (1)$$

$$\frac{ds_i}{dt} = J_{SRuptake_i} - J_{CICR_i} - J_{leak_i}, \quad (2)$$

$$\frac{dv_i}{dt} = \gamma(-J_{Na/K_i} - J_{Cl_i} - 2J_{VOCC_i} - J_{Na/Ca_i} - J_{K_i}), \quad (3)$$

$$\frac{dw_i}{dt} = \lambda(K_{activation_i} - w_i). \quad (4)$$

The various terms appearing in this set of nonlinear differential equations are detailed in Parthimos et al. (1999). The quantity J_{IP3i} represents the calcium release from the stores possessing IP_3-receptors. It then depends on the concentration of IP_3 (see Eq. 17 below). The term

$$J_{VOCC_i} = G_{Ca}\frac{v_i - v_{Ca_1}}{1 + e^{-[(v_i - v_{Ca_2})/R_{Ca}]}} \quad (5)$$

models the calcium influx through VOCCs,

$$J_{Na/Ca_i} = G_{Na/Ca}\frac{c_i}{c_i + c_{Na/Ca}}(v_i - v_{Na/Ca}) \quad (6)$$

is the Na^+/Ca^{2+} exchange,

$$J_{SRuptake_i} = B\frac{c_i^2}{c_i^2 + c_b^2} \quad (7)$$

is the SR uptake,

$$J_{CICR_i} = C\frac{s_i^2}{s_c^2 + s_i^2}\frac{c_i^4}{c_c^4 + c_i^4} \quad (8)$$

is the calcium-induced calcium release (CICR),

$$J_{extrusion_i} = Dc_i\left(1 + \frac{v_i - v_d}{R_d}\right) \quad (9)$$

is the calcium extrusion from the SMC by Ca^{2+}-ATPase pumps,

$$J_{leak_i} = Ls_i \quad (10)$$

is the leak from the SR,

$$J_{Na/K_i} = F_{Na/K} \quad (11)$$

is the Na^+-K^+-ATPase,

$$J_{\mathrm{Cl_i}} = G_{\mathrm{Cl}}(v_\mathrm{i} - v_{\mathrm{Cl}}) \tag{12}$$

is the chloride channels,

$$J_{\mathrm{K_i}} = G_{\mathrm{K}} w_\mathrm{i}(v_\mathrm{i} - v_{\mathrm{K}}) \tag{13}$$

is the K^+ efflux, and

$$K_{\mathrm{activation_i}} = \frac{(c_\mathrm{i} + c_\mathrm{w})^2}{(c_\mathrm{i} + c_\mathrm{w})^2 + \beta e^{-[(v_\mathrm{i} - v_{\mathrm{Ca_3}})/R_\mathrm{K}]}} \tag{14}$$

is the calcium and voltage activation of K^+ channels.

The meaning of the parameters is given in Table 1. The numerical values of the fixed physiological parameters are taken from Parthimos et al. (1999), as well as those of the free parameters c_b, s_c, λ, c_w, β, and γ. $c_\mathrm{b} = 1.0\ \mu$M, $s_\mathrm{c} = 2.0\ \mu$M, $\lambda = 45.0$, $c_\mathrm{w} = 0\ \mu$M, $\beta = 0.13\ \mu\mathrm{M}^2$, and $\gamma = 1970$ mV/μM. The relative amplitudes of the terms 5–14 are adjusted to reproduce the experimental (Peng et al., 2001; Lamboley et al., 2003) duration of a spike, the oscillation frequency, and the mean calcium level in response to vasoconstrictor stimulations: $G_{\mathrm{Ca}} = 0.00129\ \mu\mathrm{M\ mV^{-1}\ s^{-1}}$, $G_{\mathrm{Na/Ca}} = 0.00316\ \mu\mathrm{M\ mV^{-1}\ s^{-1}}$, $B = 2.025\ \mu$M/s, $C = 55\ \mu$M/s, $D = 0.24\ \mathrm{s^{-1}}$, $L = 0.025\ \mathrm{s^{-1}}$, $F_{\mathrm{Na/K}} = 0.0432\ \mu$M/s, $G_{\mathrm{Cl}} = 0.00134\ \mu\mathrm{M\ mV^{-1}\ s^{-1}}$, and $G_{\mathrm{K}} = 0.00446\ \mu\mathrm{M\ mV^{-1}\ s^{-1}}$. As membrane channels open and close stochastically at finite temperature, a Gaussian noise is added in the membrane conductances.

To test if IP_3 diffusion plays a role in synchronization during vasomotion, an equation describing the IP_3 dynamics is added to Eqs. 1–4 (Höfer et al., 2002),

$$\frac{dI_\mathrm{i}}{dt} = J_{\mathrm{PLC_{agonist_i}}} + J_{\mathrm{PLC\delta_i}} - J_{\mathrm{degrad_i}}, \tag{15}$$

where I_i represents the IP_3 concentration in cell i. The constant $J_{\mathrm{PLC_{agonist_i}}}$ is the rate of the PLC activated by receptor-ligand agonists, whereas the term

$$J_{\mathrm{PLC\delta_i}} = E\frac{c_\mathrm{i}^2}{K_{\mathrm{Ca}}^2 + c_\mathrm{i}^2} \tag{16}$$

models the PLC-δ. The unknown amplitude E of $J_{\mathrm{PLC\delta_i}}$ will be important for the study of intercellular IP_3 coupling, and it will be treated as a free parameter. Finally, $J_{\mathrm{degrad_i}} = kI_\mathrm{i}$ expresses IP_3 degradation. The term $J_{\mathrm{IP3_i}}$ in Eq. 1 is directly related to the IP_3 concentration (Höfer et al., 2002):

$$J_{\mathrm{IP3_i}} = F\frac{I_\mathrm{i}^2}{K_\mathrm{r}^2 + I_\mathrm{i}^2}. \tag{17}$$

The maximal rate F of activation-dependent calcium influx is set to 0.23 μM/s. With this value, J_{IP3i} is in a reasonable range for comparison with the experiments of Lamboley et al. (2003). The rate of IP_3 degradation k is set to $0.1\ \mathrm{s^{-1}}$ (Wang et al., 1995). The other parameter values are taken from Höfer et al. (2002) and are enumerated in Table 2.

TABLE 1 Parameter values for the single cell model of Parthimos et al. (1999)

Parameter	Description	Units or value if fixed
G_{Ca}	Whole cell conductance for VOCCs	$\mu\mathrm{M\ mV^{-1}\ s^{-1}}$
$v_{\mathrm{Ca_1}}$	Reversal potential for VOCCs	100.0 mV
$v_{\mathrm{Ca_2}}$	Half-point of the VOCC activation sigmoidal	−24.0 mV
R_{Ca}	Maximum slope of the VOCC activation sigmoidal	8.5 mV
$G_{\mathrm{Na/Ca}}$	Whole cell conductance for Na^+/Ca^{2+} exchange	$\mu\mathrm{M\ mV^{-1}\ s^{-1}}$
$c_{\mathrm{Na/Ca}}$	Half-point for activation of Na^+/Ca^{2+} exchange by Ca^{2+}	0.5 μM
$v_{\mathrm{Na/Ca}}$	Reversal potential for the Na^+/Ca^{2+} exchanger	−40.0 mV
B	SR uptake rate constant	μM/s
c_b	Half-point of the SR ATPase activation sigmoidal	μM
C	CICR rate constant	μM/s
s_c	Half-point of the CICR Ca^{2+} efflux sigmoidal	μM
c_c	Half-point of the CICR activation sigmoidal	0.9 μM
D	Rate constant for Ca^{2+} extrusion by the ATPase pump	$\mathrm{s^{-1}}$
v_d	Intercept of voltage dependence of extrusion ATPase	−100.0 mV
R_d	Slope of voltage dependence of extrusion ATPase	250.0 mV
L	Leak from SR rate constant	$\mathrm{s^{-1}}$
γ	Scaling factor relating net movement of ion fluxes to the membrane potential (inversely related to cell capacitance)	mV/μM
$F_{\mathrm{Na/K}}$	Net whole cell flux via the Na^+-K^+-ATPase	μM/s
G_{Cl}	Whole cell conductance for Cl^- current	$\mu\mathrm{M\ mV^{-1}\ s^{-1}}$
v_{Cl}	Reversal potential for Cl^- channels	−25.0 mV
G_{K}	Whole cell conductance for K^+ efflux	$\mu\mathrm{M\ mV^{-1}\ s^{-1}}$
v_{K}	Reversal potential for K^+	−94.0 mV
λ	Rate constant for net K_{Ca} channel opening	
c_w	Translation factor for Ca^{2+} dependence of K_{Ca} channel activation sigmoidal	μM
β	Translation factor for membrane potential dependence of K_{Ca} channel activation sigmoidal	$\mu\mathrm{M}^2$
$v_{\mathrm{Ca_3}}$	Half-point for the K_{Ca} channel activation sigmoidal	−27.0 mV
R_{K}	Maximum slope of the K_{Ca} activation sigmoidal	12.0 mV

Intercellular communication

We assume only one layer of SMCs in the arteries, i.e., we consider a two-dimensional model, in which SMCs communicate via gap junctions. As gap junctions connect adjacent cells, a cell is assumed to communicate only with its first-neighbors. SMCs are disposed as on Fig. 1. Every cell is coupled to its six first-neighbors. Gap junctions between two neighboring cells are modeled by a single global conductance or permeability, which is supposed to be the same in every direction, even if the contact surface between adjacent cells is variable. Moreover, the intercellular interactions are assumed to be symmetric as we study homocellular communications.

A term

$$V_{\mathrm{coupling_i}} = -g\sum_\mathrm{j}(v_\mathrm{i} - v_\mathrm{j}) \tag{18}$$

TABLE 2 Parameter values for the IP_3 dynamics; Höfer et al. (2002)

Parameter	Description	Value
E	Maximal rate of PLC-δ	μM/s
K_{Ca}	Half-saturation constant for calcium activation of PLC-δ	0.3 μM
k	Rate constant of IP_3 degradation	s^{-1}
K_r	Half-saturation constant for agonist-dependent calcium entry	1 μM

is added for each cell i to Eq. 3 to model the electrical coupling between cells. The gap junctional electrical coupling coefficient g is related to the gap junctional conductance G by $g = G/C_m$, where C_m is the cell membrane capacitance. The conductance G reflects the composite junctional permeability to small cytoplasmic ions (Verselis et al., 1986) between the cell i and its first-neighbors j. Setting $C_m \simeq 10^{-5}\mu$F (Parthimos et al., 1999) and $G \simeq 10$ nS (Moore et al., 1991; Moore and Burt, 1995; Li and Simard, 1999; Yamamoto et al., 2001) gives a gap junctional electrical coupling coefficient g of the order of 1000 s^{-1}.

The calcium coupling describing calcium diffusion is modeled by a term

$$J_{c-coupling_i} = -p\sum_j (c_i - c_j), \tag{19}$$

complementing Eq. 1. The parameter p is the gap junctional calcium coupling coefficient related to the gap junctional permeability P by $p = P/l$, where l represents the mean diffusion path in a cell, which is of the order of the cell width. As we have not found any values for the gap junctional permeability P of the SMCs in the literature, the coupling coefficient $p = P/l$ will be treated as a crucial free parameter.

The coupling due to IP_3 diffusion, added to Eq. 15, is described in the same manner as the calcium coupling:

$$J_{I-coupling_i} = -p_{IP_3}\sum_j (I_i - I_j). \tag{20}$$

As for p, to the best of our knowledge, there is no experimental value of the coupling coefficient p_{IP_3} for SMCs in the literature. Apart from the fact that $p \ll p_{IP_3}$ (as the effect of fast calcium buffering is included in p; Höfer et al., 2001), p_{IP_3} is a free parameter.

Variability in a population of SMCs

As shown in Hamada et al. (1997), freshly dispersed SMCs stimulated with a sufficiently high concentration of PE oscillate at similar frequencies. That is the reason why the parameter values are taken the same for all cells. Only the Gaussian noise in the membrane conductance parameter values (stochastic opening and closing of channels) induces some variability in the response of different cells. The noise level is chosen to obtain comparable variances for model curves and experimental data (Lamboley et al., 2003).

Vasoconstrictor stimulation

Receptor-ligand agonists like PE or NE are used to induce calcium rises: After binding on cell-surface receptors (PE binds to α-adrenoceptors, and NE to α- and β-adrenoceptors), they activate phospholipase C (PLC) and induce the release of IP_3. IP_3 then releases calcium from the SR (Minneman, 1988). A raise in the receptor-ligand agonist concentration is simulated by an increase of the PLC rate $J_{PLC_{agonist_i}}$.

Extracellular KCl does not directly produce the intracellular cascades arising with receptor-ligand activation. As KCl changes the Nernst potentials for K^+ and Cl^-, it acts by depolarizing the cell membrane of the SMCs, opening VOCCs (Nelson et al., 1990). An increase in the KCl concentration is simulated by changing the reversal potential of K^+ and Cl^- (v_K and v_{Cl}) in Eq. 3, accordingly to the Nernst equation.

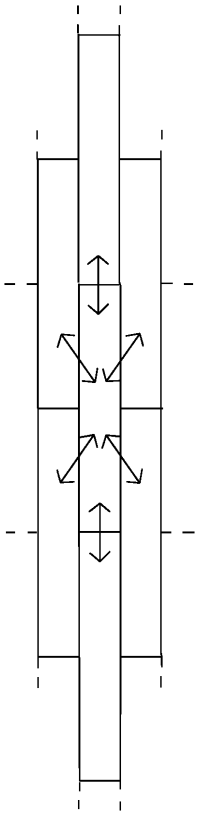

FIGURE 1 The model equations are integrated on a two-dimensional grid of SMCs. As the typical size of a single SMC is 5 μm $\times$ 50 μm, the cell geometry is approximated by a rectangle. Dimensions of the cells are assumed for visualization and do not affect the intercellular coupling. Each SMC is generally connected with six neighbors (*arrows*).

Numerical methods

Using a fourth-order Runge-Kutta method, the model equations were integrated on a two-dimensional grid of ~90 rectangular cells (Fig. 1). A cell has six first-neighbors, or less if it is situated near the border. Within each cell, the calcium and membrane potential dynamics are described by Eqs. 1–4 and 15. (Movies of the simulations showing the evolution of the calcium concentration on this two-dimensional grid are available in the Supplementary Material.) Moreover, to complete our analysis, we used the softwares XPP and AUTO, as implemented in XPPAUT by B. Ermentrout (*http://www.pitt.edu/~phase/*): the equations in the case of one and two coupled cells were solved with XPP and AUTO was used for bifurcation diagrams. All stable parts of branches indicated by AUTO have been found in our numerical simulations.

RESULTS

Receptor-ligand agonist stimulation

Single SMC behavior

The behavior of the cytosolic calcium concentration c_i with respect to the agonist-activated PLC-rate $J_{PLC_{agonist_i}}$ (which is directly related to the vasoconstrictor concentration) is shown on Fig. 2 *a*. In this figure, the amplitude E of the rate of PLC-δ is set to zero, and no noise is introduced in the conductance parameters. Increasing the parameter $J_{PLC_{agonist_i}}$, one reaches a Hopf bifurcation at $J_{PLC_{agonist_i}} = 0.067\,\mu M/s$. Thus in absence of noise, the cytosolic calcium level is in a stable steady state (subthreshold behavior) at low agonist concentrations ($J_{PLC_{agonist_i}} < 0.067\,\mu M/s$),whereas at higher concentrations ($J_{PLC_{agonist_i}} > 0.067\,\mu M/s$) the calcium level oscillates. With increasing agonist concentrations, the mean calcium level and the frequency of the oscillations become higher, whereas the amplitude of the oscillations is slightly decreasing. A Hopf bifurcation at $J_{PLC_{agonist_i}} = 0.149\,\mu M/s$ leads to a state with a high sustained calcium level that no longer oscillates.

Introducing a Gaussian noise in the channel conductances results in few irregular flashings of the SMC in the subthreshold state (Fig. 2 *b*). The calcium level may exceed a threshold and flash at moments distributed stochastically in time. Actually, noise induces variations in parameter values, changes the bifurcation diagram, and shifts the Hopf bifurcation. So, if at a certain moment the Hopf bifurcation point is moved sufficiently in the proper direction, a calcium flash occurs. As the parameter values vary stochastically, these flashings are irregular. Raising $J_{PLC_{agonist_i}}$ increases the calcium level and thus the probability of flashing.

Introduction of noise at higher values of $J_{PLC_{agonist_i}}$ ($J_{PLC_{agonist_i}} > 0.067\,\mu M/s$) results in little fluctuations between two calcium rises and in small variations in the amplitude of the peaks (Fig. 2, *c* and *d*).

Increasing the amplitude E of the rate of PLC-δ does not change the shape of the bifurcation diagram presented on Fig. 2 *a*. However, the diagram is shifted so that the Hopf bifurcations occur for smaller values of $J_{PLC_{agonist_i}}$. For $E > 0.12\ \mu M/s$, the first Hopf bifurcation is before $J_{PLC_{agonist_i}} = 0$, i.e., the cell is oscillating even in absence of a vasoconstrictor. This is in contradiction with experimental data and values of $E > 0.12\ \mu M/s$ can then be excluded.

The time courses of all variables for $J_{PLC_{agonist_i}} = 0.078\,\mu M/s$ are given on Fig. 3. An elevation in cytosolic calcium concentration is preceded by a membrane depolarization that allows calcium influx through VOCCs. Increasing cytosolic calcium level decreases the calcium concentration in the SR, and increases the open state probability of calcium-activated potassium channels which brings about a membrane hyperpolarization. If the amplitude E of PLC-δ is nonzero, the IP_3 level follows the oscillation of

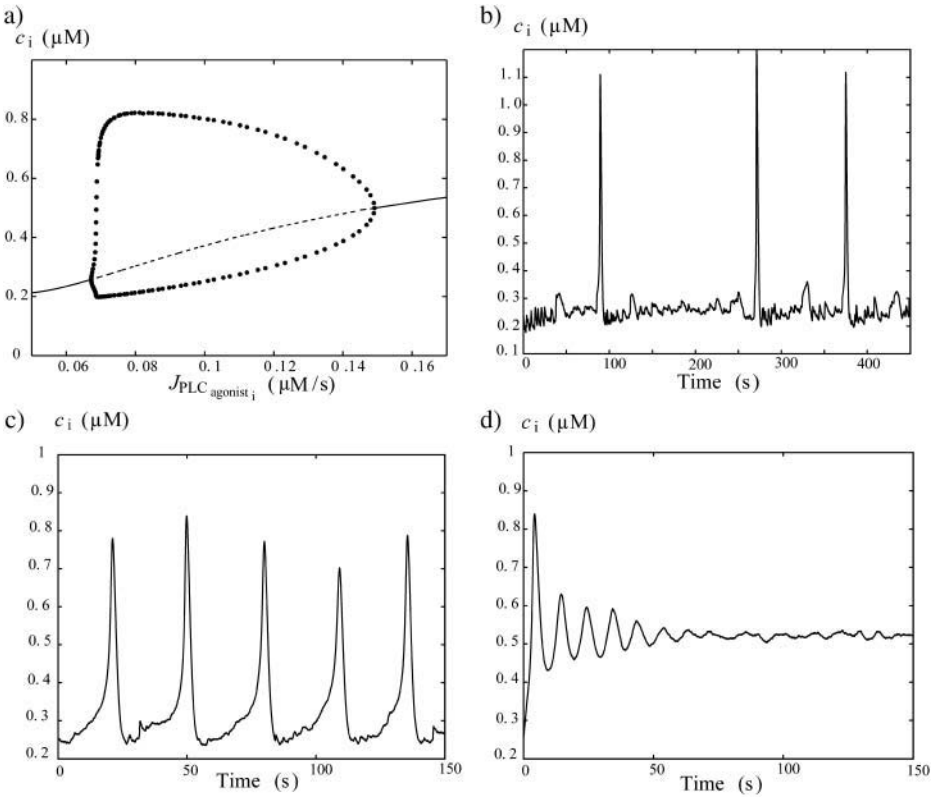

FIGURE 2 (*a*) Bifurcation diagram for the cytosolic calcium concentration c_i of an isolated SMC stimulated by a receptor-ligand agonist (*solid line*, stable rest state; *dashed line*, unstable rest state; and ●, minima and maxima of stable oscillations). The amplitude E of the PLC-δ rate is set to zero, and no noise in the conductance parameters is introduced. At low values of $J_{PLC_{agonist_i}}$ (i.e., at low agonist concentrations), the cytosolic calcium level is in a stable steady state. At $J_{PLC_{agonist_i}} = 0.067\,\mu M/s$, a Hopf bifurcation occurs; the steady state becomes unstable and the calcium concentration begins to oscillate. At $J_{PLC_{agonist_i}} = 0.149\,\mu M/s$, there is a Hopf bifurcation and the steady state becomes stable again. Panels *b*, *c*, and *d* give the evolution of the cytosolic calcium concentration of an isolated cell in presence of noise for three values of $J_{PLC_{agonist_i}}$: (*b*) $J_{PLC_{agonist_i}} = 0.06\,\mu M/s$; irregular flashings due to noise. (*c*) $J_{PLC_{agonist_i}} = 0.08\,\mu M/s$; oscillations. (*d*) $J_{PLC_{agonist_i}} = 0.165\,\mu M/s$; oscillations converging to the stable steady state.

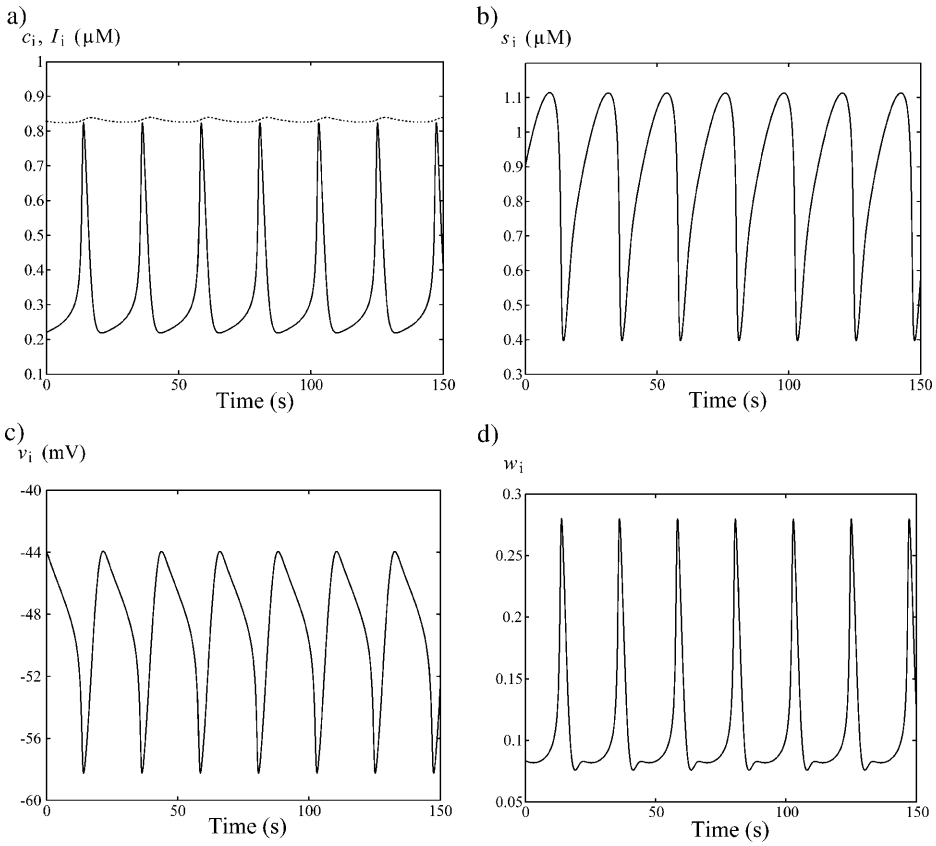

FIGURE 3 Time courses of all model variables for an isolated SMC stimulated by a receptor-ligand agonist ($J_{\mathrm{PLC}_{\mathrm{agonist}_i}} = 0.078\,\mu\mathrm{M/s}$). No noise is introduced. The amplitude E of PLC-δ is set to 0.01 μM/s, which gives rise to low amplitude IP_3 oscillations. (*a*, *solid line*, cytosolic calcium concentration c_i; and *dotted line*, IP_3 concentration I_i (stationary). (*b*) Calcium concentration in the SR s_i. (*c*) Cell membrane potential v_i. (*d*) Open state probability of calcium activated potassium channels w_i.

cytosolic calcium concentration. Increasing E increases the amplitude of IP_3 oscillations.

Population of coupled SMCs

Effects of electrical coupling. The values of the coupling coefficients p and p_{IP_3} are set to zero to analyze only the effects of electrical coupling. Our simulations show that an electrical coupling is not able to synchronize calcium oscillations at all vasoconstrictor concentrations. A bifurcation diagram of the calcium concentration in the case of two electrically coupled cells ($g = 1000\ \mathrm{s}^{-1}$) is given on Fig. 4 *a*. The Hopf bifurcations at $J_{\mathrm{PLC}_{\mathrm{agonist}_i}} = 0.067\,\mu\mathrm{M/s}$ and $J_{\mathrm{PLC}_{\mathrm{agonist}_i}} = 0.149\,\mu\mathrm{M/s}$ are at the same position as for the single cell bifurcation diagram (Fig. 2 *a*). The branch of periodic orbits emanating from them has become unstable, except for the ranges $0.0689\,\mu\mathrm{M/s} < J_{\mathrm{PLC}_{\mathrm{agonist}_i}} < 0.0691\,\mu\mathrm{M/s}$ and $0.130\,\mu\mathrm{M/s} < J_{\mathrm{PLC}_{\mathrm{agonist}_i}} < 0.147\,\mu\mathrm{M/s}$. This mostly unstable branch corresponds to synchronous calcium oscillations, during which membrane potential and calcium concentration oscillate in phase at the same frequency. With respect to the single cell bifurcation diagram there are two additional Hopf bifurcations occurring at $J_{\mathrm{PLC}_{\mathrm{agonist}_i}} = 0.061\,\mu\mathrm{M/s}$ and $J_{\mathrm{PLC}_{\mathrm{agonist}_i}} = 0.151\,\mu\mathrm{M/s}$. They give rise to an essentially stable branch of periodic orbits. This branch corresponds to synchronous membrane potentials associated to regular asynchronous calcium oscillations. This means that calcium oscillations are out of phase, but each calcium oscillation brings about a membrane potential oscillation in the other cell. Thus membrane potential oscillates twice whereas calcium oscillates only once. As the Hopf bifurcation $J_{\mathrm{PLC}_{\mathrm{agonist}_i}} = 0.061\,\mu\mathrm{M/s}$ is occurring before the first Hopf bifurcation (at $J_{\mathrm{PLC}_{\mathrm{agonist}_i}} = 0.067\,\mu\mathrm{M/s}$) in the single cell bifurcation diagram, oscillations are generated by electrical coupling: electrically coupled SMCs in the subthreshold state (for $0.061\,\mu\mathrm{M/s} < J_{\mathrm{PLC}_{\mathrm{agonist}_i}} < 0.067\,\mu\mathrm{M/s}$) present asynchronous calcium oscillations, although the cells taken separately are nonoscillating and flash only from time to time. The oscillations are periodic, even in the region between the first Hopf bifurcation at $J_{\mathrm{PLC}_{\mathrm{agonist}_i}} = 0.061\,\mu\mathrm{M/s}$ and the first occurrence of stable oscillatory solutions on the bifurcation diagram of Fig. 4 *a*. If one increases the number of coupled SMCs we still observe the generation of oscillations and simultaneous out-of-phase calcium concentration and in-phase membrane potential oscillations of neighboring cells (see Fig. 5 in the case of three cells). Intuitively the generation of oscillations can be explained in the following way: when one cell is flashing in the subthreshold state, the neighboring cell prevents it from having large membrane potential oscillation during this calcium spike, which perturbates its calcium dynamics. For example, the amplitude of the calcium-induced membrane

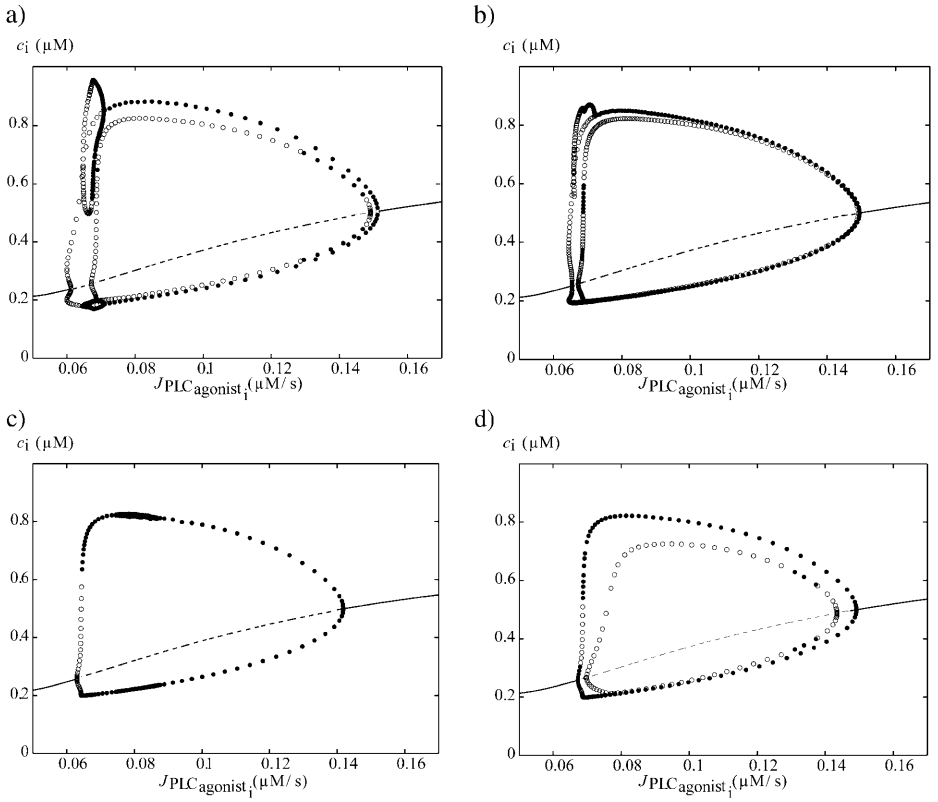

FIGURE 4 Bifurcation diagrams for the cytosolic calcium concentration c_i of an SMC stimulated by a receptor-ligand agonist in the case of two coupled cells (*solid line*, stable rest state; *dashed line*, unstable rest state; ●, minima and maxima of stable oscillations; and ○, minima and maxima of unstable oscillations). The amplitude E of the PLC-δ rate is set to zero in *a*, *b*, and *d*, and no noise in the conductance parameters is introduced. (*a*) Electrical coupling ($g = 1000\ s^{-1}$, $p = p_{IP_3} = 0\ s^{-1}$). There are four Hopf bifurcations at $J_{PLC_{agonist_i}} = 0.061\ \mu M/s$, $J_{PLC_{agonist_i}} = 0.067\ \mu M/s$, $J_{PLC_{agonist_i}} = 0.149\ \mu M/s$, and $J_{PLC_{agonist_i}} = 0.151\ \mu M/s$. (*b*) Electrical coupling ($g = 1\ s^{-1}$, $p = p_{IP_3} = 0\ s^{-1}$). With respect to the bifurcation diagram in *a*, the external Hopf bifurcations have been shifted toward the bifurcations at $J_{PLC_{agonist_i}} = 0.067\ \mu M/s$ and $J_{PLC_{agonist_i}} = 0.149\ \mu M/s$. They are now at $J_{PLC_{agonist_i}} = 0.065\ \mu M/s$ and $J_{PLC_{agonist_i}} = 0.150\ \mu M/s$. (*c*) IP_3 coupling ($p_{IP_3} = 1\ s^{-1}$, $E = 0.01\ \mu M/s$, $g = p = 0\ s^{-1}$). The Hopf bifurcations at $J_{PLC_{agonist_i}} = 0.063\ \mu M/s$ and $J_{PLC_{agonist_i}} = 0.142\ \mu M/s$ are at the same position as for the single cell bifurcation diagram at this value of E. (*d*) Calcium coupling ($p = 0.03\ s^{-1}$, $g = p_{IP_3} = 0\ s^{-1}$). There are four Hopf bifurcations at $J_{PLC_{agonist_i}} = 0.067\ \mu M/s$, $J_{PLC_{agonist_i}} = 0.070\ \mu M/s$, $J_{PLC_{agonist_i}} = 0.143\ \mu M/s$, and $J_{PLC_{agonist_i}} = 0.149\ \mu M/s$.

potential hyperpolarization is then smaller than for an isolated cell, the calcium influx through VOCCs is less decreased during hyperpolarization, and thus the cytosolic calcium level may become higher and begin to oscillate. This is only possible for out-of-phase calcium oscillations, as one cell has to damp the membrane potential oscillations of the other cell.

Decreasing g shifts the two additional Hopf bifurcations toward the Hopf bifurcations at $J_{PLC_{agonist_i}} = 0.067\ \mu M/s$ and $J_{PLC_{agonist_i}} = 0.149\ \mu M/s$ (Fig. 4 *b*). We observe that the out-of-phase effect on calcium oscillations is more important at high values of g ($g \geq 10\ s^{-1}$) for which membrane potential oscillations are synchronous. Indeed, as the membrane potential oscillates in phase with the calcium concentration in a single cell and electrical coupling produces out-of-phase calcium oscillations of several cells, a sufficiently high value of g is needed to synchronize membrane potential oscillations.

Effects of IP_3 coupling. First the values of the coupling coefficients g and p are set to zero to analyze only the effects of IP_3 coupling. The bifurcation diagram for an individual cell is not significantly changed by an increase of the coupling coefficient p_{IP_3}. For a given amplitude E of the PLC-δ the Hopf bifurcations are at the same position as for the single cell bifurcation diagram. The essentially stable branch of periodic solutions emanating from them corresponds to synchronous calcium oscillations (see Fig. 4 *c* for the case $p_{IP_3} = 1\ s^{-1}$ and $E = 0.01\ \mu M/s$). Thus IP_3 coupling has a synchronizing effect on calcium oscillations. This effect becomes more significant with high values of p_{IP3} and of the amplitude E of the PLC-δ.

If $g = 1000\ s^{-1}$, an IP_3 coupling coefficient $p_{IP_3} > 1\ s^{-1}$ is needed to synchronize IP_3 oscillations. But these synchronous IP_3 oscillations alone cannot synchronize calcium oscillations for reasonable values of E (i.e., for $0\ \mu M/s \leq E \leq 0.12\ \mu M/s$), whatever value of p_{IP_3} is used. This is due to the fact that the amplitude of the IP_3 oscillations is small (Fig. 3 *a*), which entails that the coupling between the IP_3 and calcium oscillations is too weak. Therefore IP_3 oscillations can be synchronous, without being able to synchronize calcium oscillations. Only for very high values of E ($E > 0.9\ \mu M/s$) is IP_3 coupling able to synchronize the calcium oscillations.

Effects of calcium coupling. If the coupling coefficients g and p_{IP_3} are set to zero, increasing p does not significantly change the stable parts of the bifurcation diagram and the frequency of oscillations compared to those of an isolated cell. The Hopf bifurcations at $J_{PLC_{agonist_i}} = 0.067\ \mu M/s$ and $J_{PLC_{agonist_i}} = 0.149\ \mu M/s$ (see Fig. 4 *d* for the case of $p = 0.03\ s^{-1}$) are at the same position as for the single cell bifurcation diagram (Fig. 2 *a*). The essentially stable branch of periodic orbits emanating from them corresponds to synchronous calcium oscillations. For the parameter range

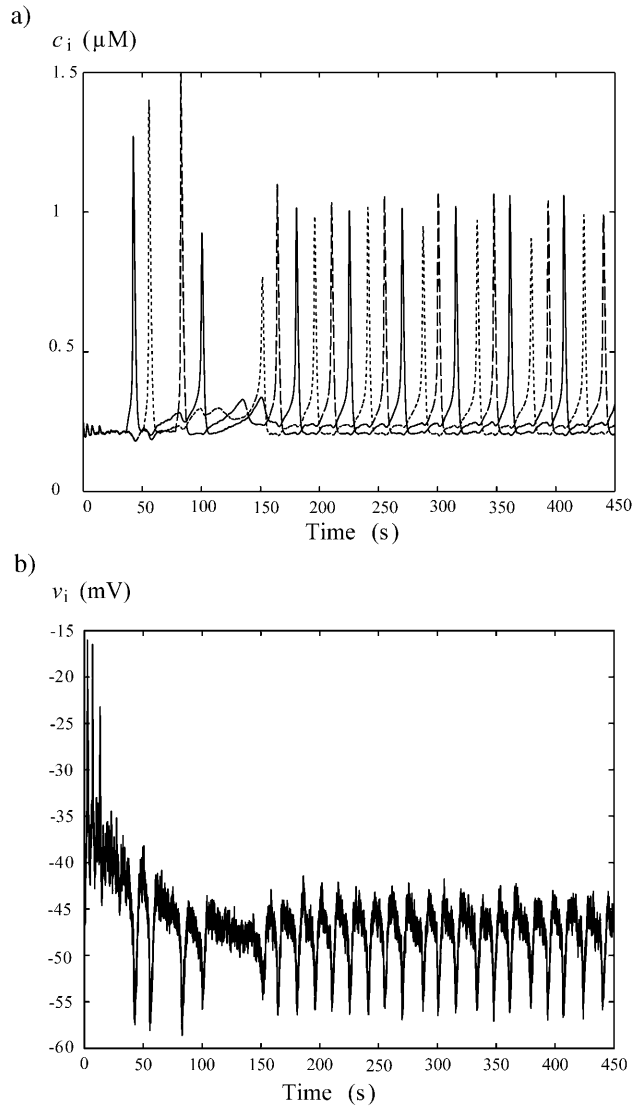

FIGURE 5 Evolution of the cytosolic calcium concentration c_i and of the membrane potential v_i in the case of three mutually electrically coupled cells (with $g = 1000\ s^{-1}$ and $p = p_{IP_3} = 0\,s^{-1}$) in the subthreshold state ($J_{PLC_{agonist_i}} = 0.064\,\mu M/s$): (*a*) regular asynchronous calcium oscillations and (*b*) synchronous membrane potential oscillations are generated. This situation corresponds to a frequency locking 3:1 (i.e., in one SMC, the membrane potential oscillates three times, whereas the calcium concentration oscillates only once).

$0.01\ s^{-1} < p < 0.18\ s^{-1}$, two additional Hopf bifurcations appear. They give rise to a mostly unstable branch of periodic solutions corresponding to antiphase calcium oscillations. Thus unlike electrical coupling, calcium coupling may synchronize calcium oscillations at every value of $J_{PLC_{agonist_i}}$.

Setting g to $1000\ s^{-1}$, a calcium coupling coefficient p above $0.03\ s^{-1}$ is needed to synchronize oscillating cells, independently of the IP_3 coupling. So a minimal calcium diffusion is necessary to a synchronization.

With a calcium coupling coefficient $0.03\ s^{-1} \le p \le 1\ s^{-1}$, the calcium flashings are not able to synchronize in the subthreshold state and the cells only flash from time to time in an irregular way. The mean calcium level over the whole grid is low and constant in time as in Fig. 6 *a*. Using a calcium permeability in the same range at higher values of $J_{PLC_{agonist_i}}$ ($J_{PLC_{agonist_i}} > 0.067\,\mu M/s$), our simulations show a perfect synchronization of the oscillations and a recruitment of all cells, independently of the initial conditions: even if the drug does not arrive simultaneously on all SMCs and the cells do not begin to oscillate at the same time, the SMCs become rapidly synchronized. The mean calcium level is then oscillating too (Fig. 6, *b* and *c*).

A calcium coupling coefficient $>1\ s^{-1}$ induces a synchronized calcium concentration in all cells in the subthreshold state, and no more asynchronous flashing is possible.

KCl stimulation

Single SMC behavior

The behavior of the cytosolic calcium concentration c_i of a single cell with respect to the KCl concentration is shown on Fig. 7 *a*. In this figure, no noise is introduced in the conductance parameters. Below the Hopf bifurcation at 9.67 mM, the SMC is in a stable steady state. Taking noise into account gives rise to irregular flashings (Fig. 7 *b*). At higher concentrations, there is a single calcium peak followed by small oscillations (Fig. 7 *c*). The membrane potential v_i oscillates in phase with c_i. The amplitude of the calcium peak is higher and its slope steeper with increasing KCl concentrations. At KCl concentrations above 15.95 mM (Hopf bifurcation), these small oscillations are abolished and only noise fluctuations remain (Fig. 7 *d*). For KCl concentrations higher than 15.95 mM, the cell response remains the same, because the value of the steady-state calcium level is no longer changing (Fig. 7 *a*).

In the subthreshold state the flashings are more irregular with KCl stimulations ([KCl] $<$ 9.67 mM), than with receptor-ligand agonist stimulations ($J_{PLC_{agonist_i}} < 0.067\,\mu M/s$).

Population of coupled SMCs

The calcium coupling coefficient p is set again to $0.03\ s^{-1}$, p_{IP_3} to zero, and g to $1000\ s^{-1}$. At low KCl concentrations ([KCl] $\le$ 9.67 mM), the behavior is similar to that observed with receptor-ligand agonist stimulations: individual SMCs are not able to synchronize their cytosolic calcium concentrations and only flash from time to time in an irregular way (Fig. 8 *a*). At higher KCl concentrations (9.67 mM $\le$ [KCl] $\le$ 15.95 mM), the first calcium peak is simultaneous for all cells (it occurs at the moment of the arrival of KCl) and is followed by asynchronous low amplitude oscillations (Fig. 8, *b* and *c*). These oscillations synchronize only for a calcium coupling coefficient $p > 1\ s^{-1}$. Above a certain KCl

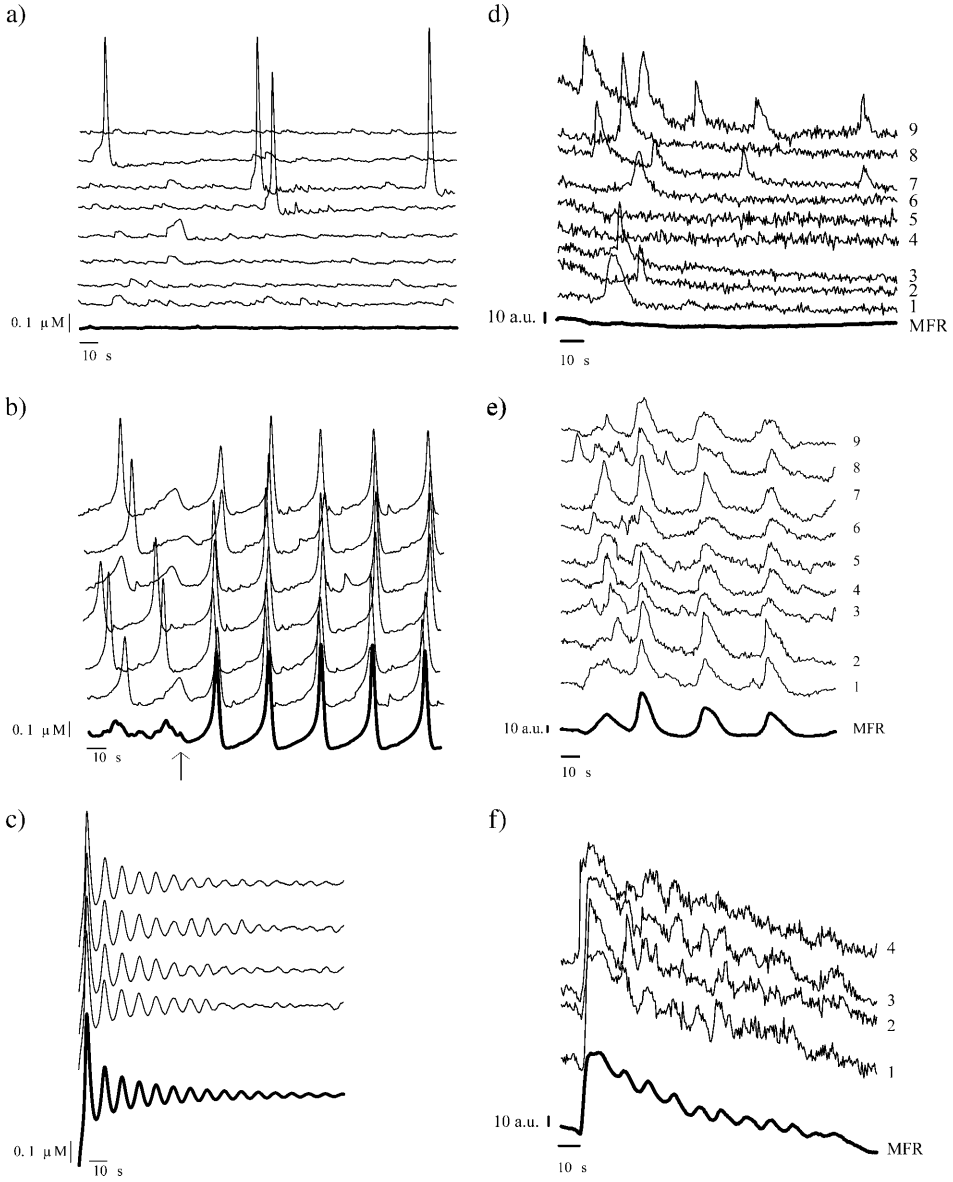

FIGURE 6 Comparison of our model with experimental data of rat mesenteric arterial strips stimulated by PE (Lamboley et al., 2003). On the left, the cytosolic calcium dynamics of several coupled SMCs is calculated (with $p = 0.03\ s^{-1}$, $g = 1000\ s^{-1}$, and $p_{IP_3} = 0$) for three values of $J_{PLC_{agonist_i}}$ (simulating low, medium, and high PE concentrations): (*a*) $J_{PLC_{agonist_i}} = 0.06\,\mu M/s$, (*b*) $J_{PLC_{agonist_i}} = 0.08\,\mu M/s$, and (*c*) $J_{PLC_{agonist_i}} = 0.165\,\mu M/s$. On the right are the corresponding experimental results obtained by measuring fluorescence ratios: (*d*) [PE] = 0.2 μM, (*e*) [PE] = 0.6 μM, and (*f*) [PE] = 1.5 μM. Each thin curve gives the evolution of the calcium concentration (*a, b*, and *c*) or fluorescence ratio (*d, e*, and *f*) in a typical SMC. The thick curve represents the mean calcium concentration/mean fluorescence ratio (*MFR*) taken over the whole grid (~80–90 cells). The three concentrations give rise to three different behaviors: (*a* and *d*) Few irregular asynchronous flashings occur and the mean value is constant and low. (*b* and *e*) There is a recruitment and a synchronization of all cells, independently of the initial conditions. The arrow indicates the beginning of the coupling. The mean calcium level is oscillating. (*c* and *f*) The mean calcium level is high; the cells are oscillating synchronously, converging to a stable steady state. On *f* the mean calcium level decreases during maintained exposure to PE. This is probably due to receptor desensitization and photobleaching. These effects are not taken into account in our model.

concentration ([KCl] > 15.95 mM), only the first peak and small noise fluctuations remain.

DISCUSSION

Recruitment of SMCs

In the subthreshold state, increasing the vasoconstrictor concentration raises the probability of flashing of a single cell, thus leading to a higher number of recruited SMCs. Many authors (Ruehlmann et al., 2000; Zang et al., 2001; Lamboley et al., 2003) have observed that the number of cells flashing in an all-or-none fashion increases with increasing vasoconstrictor concentrations, until a concentration, for which all cells are subject to calcium rises. In our model this threshold vasoconstrictor concentration corresponds to the Hopf bifurcation.

Electrical coupling

As Savineau and Marthan (2000) reviewed, the behavior of isolated SMCs in response to agonist stimulations is variable: some types of SMCs present calcium oscillations, whereas others present only a transient calcium increase. An interesting result of our model is that synchronous membrane potential and asynchronous calcium oscillations can be generated when isolated cells in the subthreshold state (i.e., nonoscillating isolated cells) are electrically coupled (Fig. 4, *a* and *b*, and Fig. 5). In our model, the asynchronous calcium oscillations reported by Ruehlmann et al. (2000) and Zang et al. (2001) are not only due to a too-weak gap junctional

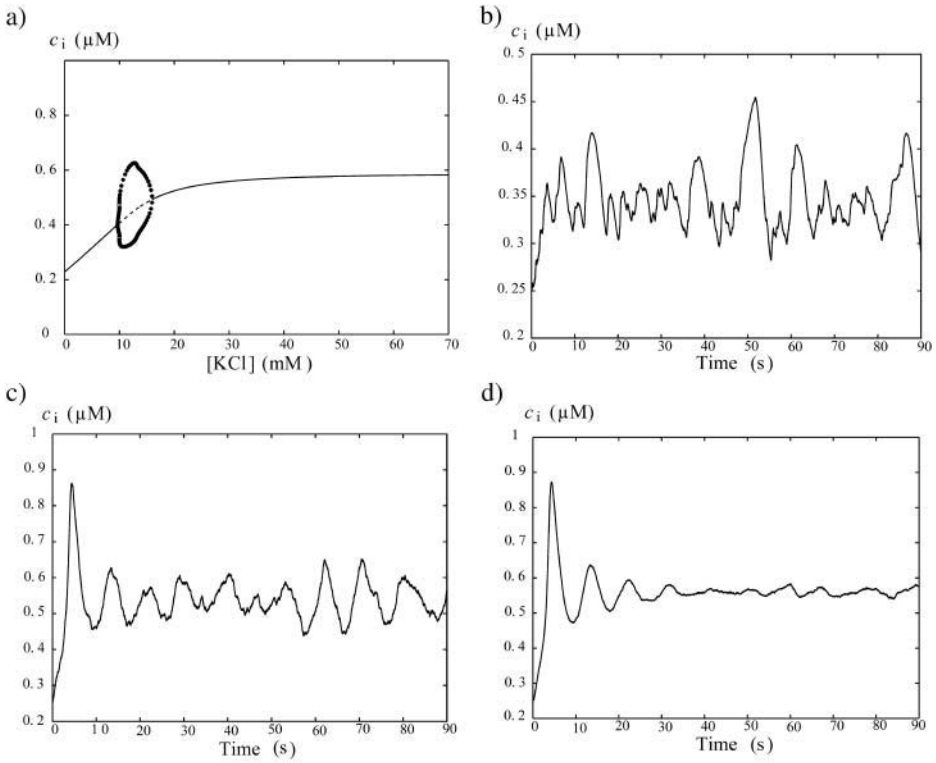

FIGURE 7 (*a*) Bifurcation diagram for the cytosolic calcium concentration c_i of an isolated SMC stimulated by KCl (*solid line*, stable rest state; *dashed line*, unstable rest state; and ●, minima and maxima of stable oscillations). At low KCl concentrations, the calcium level is in a stable steady state. At [KCl] = 9.67 mM, a Hopf bifurcation occurs and low amplitude calcium oscillations appear. At [KCl] = 15.95 mM, there is a Hopf bifurcation and the steady state becomes stable again. Panels *b*, *c*, and *d* give the evolution of the cytosolic calcium concentration of an isolated SMC in presence of noise for three values of [KCl]: (*b*) [KCl] = 5 mM; irregular flashings due to noise. (*c*) [KCl] = 15 mM; oscillations. (*d*) [KCl] = 50 mM; fluctuations due to noise.

coupling, as one might intuitively expect, but to a strong electrical coupling as well.

IP_3 coupling

As a PLC-δ has been detected in many types of SMCs, which entails that calcium oscillations give rise to IP_3 oscillations, it is worthwhile to test if IP_3 coupling can synchronize calcium oscillations. The hypothesis was plausible as IP_3 diffuses much faster and has a greater gap junctional permeability than calcium.

However, our simulations have shown that PLC-δ amplitudes $E < 0.12$ μM/s must be considered. In the case of astrocytes, Höfer et al. (2002) have even deduced that E must be <0.05 μM/s, as $E > 0.05$ μM/s leads to regenerative intercellular calcium waves that have no limit in the length of propagation (a fact that is not observed experimentally). For values of $E < 0.12$ μM/s, our results show that, for a permeability to IP_3 as high as possible, no synchronization of calcium oscillations could be achieved by IP_3 diffusion alone.

Calcium coupling

A calcium coupling is needed to obtain a synchronization of calcium oscillations at all vasoconstrictor concentrations. This allows us to set a minimal value $p_{min} = 0.03$ s^{-1} for the gap junctional calcium coupling coefficient. As the flashings observed in vitro are asynchronous in the subthreshold state, a maximal value of the calcium coupling coefficient ($p_{max} = 1$ s^{-1}) can also be deduced from our model. This value corresponds to the maximal value that can be used to obtain small asynchronous calcium oscillations under KCl stimulation. Assuming a mean intracellular calcium diffusion path of 5 μm, the minimal calcium permeability needed for synchronization can be deduced: $P_{min} = 0.15$ μm/s. To the best of our knowledge, there is no value for P in the literature, but our range encompasses the calcium permeability deduced in other theoretical models describing homocellular calcium communication: for hepatocytes, the estimations of Wilkins and Sneyd (1998) and Höfer (1999) are, respectively, $P = 0.1$ μm/s and $P = 0.6$ μm/s.

Electrical coupling and IP_3 diffusion are not sufficient to synchronize the calcium oscillations of a population of stimulated cells. However, it is worth noticing that through these couplings a stimulated cell could give rise to an intercellular calcium wave that propagates to several non-stimulated neighboring cells. For example, an intercellular calcium wave in epithelial cells has been modeled assuming only intercellular IP_3 diffusion (Sneyd et al., 1995). Note that the diffusion coefficient and the permeability for IP_3 are much larger than for calcium. An intercellular calcium wave that propagates through calcium diffusion can therefore be very slow compared to a wave that propagates through IP_3 diffusion (Höfer et al., 2002). So a weak calcium permeability $P = 0.15$ μm/s is sufficient to synchronize

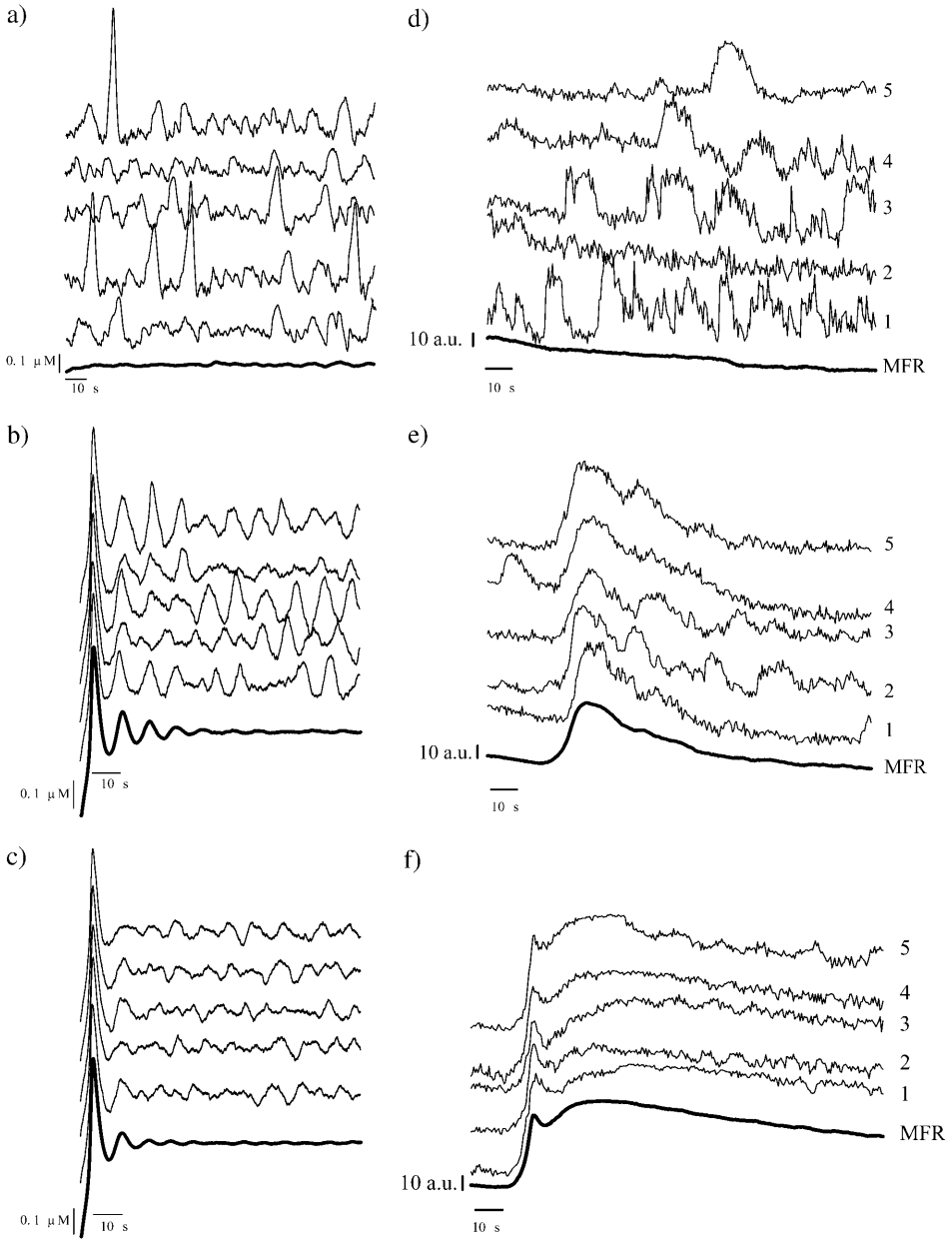

FIGURE 8 Comparison of our model with experimental data of rat mesenteric arterial strips stimulated by KCl (Lamboley et al., 2003). On the left, the cytosolic calcium dynamics of several coupled SMCs is calculated (with $p = 0.03\ s^{-1}$, $g = 1000\ s^{-1}$, and $p_{IP_3} = 0$). On the right are the corresponding experimental results obtained by measuring fluorescence ratios. Each thin curve gives the evolution of the calcium concentration/fluorescence ratio in a typical SMC. The thick curve represents the mean calcium concentration/mean fluorescence ratio (*MFR*) taken over the whole grid (~80–90 cells). Low, medium, and high KCl concentrations give rise to three different behaviors: (*a*) [KCl] = 5 mM and (*d*) [KCl] = 0.5 mM (the same behavior is observed in Lamboley et al., 2003, for 0.5 mM ≤ [KCl] ≤ 10 mM): irregular asynchronous flashings occur and the mean value is constant and low. (*b* and *e*) [KCl] = 15 mM: the first peak is followed by low amplitude asynchronous calcium oscillations. The mean value of these asynchronous oscillations is constant. (*c* and *f*) [KCl] = 50 mM: the first peak is followed by a sustained calcium level that is no longer oscillating.

oscillating cells, whereas it can be too weak to obtain fast waves.

Discussion of the model hypotheses

To describe the calcium dynamics in a single SMC, we have chosen to extend the model of Parthimos et al. (1999), which is, to the best of our knowledge, the most advanced model of SMCs. Our explanations of the recruitment and irregular asynchronous flashings rely only on the presence of an oscillation threshold (like a Hopf bifurcation), provided some noise is introduced in the model. We have also noticed that regular asynchronous calcium oscillations can be generated in the subthreshold state when cells are electrically coupled. This is due to the presence of two additional Hopf bifurcations giving rise to an essentially stable branch of periodic orbits. A comparable behavior would be observed in any SMC model that would consist of an intracellular calcium oscillator coupled to some equations describing the cell membrane potential dynamics. The contribution of VOCCs is crucial: If one SMC is flashing in the subthreshold state, the neighboring SMCs prevent it from having a large membrane potential hyperpolarization. The calcium influx through VOCCs is then less decreased, and this rises the calcium level, destabilizes the steady state of the intracellular oscillator, and brings about oscillations.

We have made the approximation that all cells are described by the same parameter values. The variability is

introduced by a Gaussian noise mimicking stochastic opening and closing of membrane channel conductances. Giving different parameter values to different cells would produce different intrinsic frequencies, and a higher minimal value for the permeability would be required to synchronize oscillating cells (Höfer, 1999). However, our hypothesis is reasonable, because freshly dispersed SMCs oscillate with similar frequencies (Hamada et al., 1997).

The gap junctional couplings are assumed to be isotropic, because no studies showing any preferential direction of wave propagation between SMCs have been found in the literature. We could have supposed that the number of gap junctions, and therefore the gap junctional coupling coefficients, are proportional to the contact surface of adjacent cells. Besides, as noise in the membrane channel conductances is included, it could also be introduced in the gap junctional coupling coefficients. We checked that these changes are not affecting the general behavior of our simulations.

As vasomotion has been observed in absence of an intact endothelium (Haddock et al., 2002; Lamboley et al., 2003), endothelial cells are not included in our model. However, several studies claim that the endothelium can play a role during vasomotion (Shimamura et al., 1999; Sell et al., 2002) and heterocellular communication between SMCs and ECs has been reported (Budel et al., 2001; Schuster et al., 2001; Dora et al., 2003). Thus it can be worth studying the heterocellular communication between SMCs and ECs. This needs further investigation and is beyond the scope of the present study.

Comparison with experiments

The model is compared to the experiments of Lamboley et al. (2003) performed on rat mesenteric arterial strips stimulated by the vasoconstrictors PE and KCl at low, medium, and high concentrations. In our simulations, a weak calcium coupling coefficient $p = 0.03\ s^{-1}$ and an electrical coupling coefficient $g = 1000\ s^{-1}$ are assumed.

For receptor-ligand agonist stimulations, the three behaviors described in Lamboley et al. (2003) are observed. At low PE concentrations ([PE] $< 0.4\ \mu M$), the mean calcium level is low and constant, and there are only irregular asynchronous flashings (Fig. 6 *d*). We suppose that these flashings originate from stochastic opening and closing of membrane channels, as modeled on Fig. 6 *a*. A weak calcium coupling coefficient such as $0.03\ s^{-1}$ is not able to synchronize them. However, sometimes a flashing in one cell brings about a flashing in a neighboring one, in agreement with the experimental results of M. Lamboley, A. Schuster, J.-L. Bény, and J.-J. Meister (unpublished results). At medium PE concentrations ($0.4\ \mu M \leq$ [PE] $\leq 0.8\ \mu M$), a recruitment and a synchronization of the oscillations of all cells are observed in vitro (Fig. 6 *e*), as simulated on Fig. 6 *b*. At high concentrations of PE ([PE] $> 0.8\ \mu M$), the cells have a sustained calcium level and oscillate rapidly (Fig. 6, *f* and *c*). The frequency of the oscillations is of the same order as in our model.

For KCl stimulations, the three behaviors observed in vitro are also obtained. At low KCl concentrations ([KCl] < 9.67 mM), there are asynchronous flashings which are more irregular than in the case of PE stimulation (Fig. 8, *a* and *d*). At medium KCl concentrations ($9.67\ mM \leq$ [KCl] ≤ 15.95 mM), our simulations present one great calcium peak followed by small asynchronous oscillations and the mean calcium level is not oscillating (Fig. 8 *b*). This is similar to the experimental results (Fig. 8 *e*). At high concentrations ([KCl] > 15.95 mM), the simulations show a peak followed by a sustained calcium level (Fig. 8 *c*) in agreement with the experiments (Fig. 8 *f*). Lamboley et al. (2003) observed that stimulating the SMCs with higher KCl concentrations than 30 mM does not change the behavior of the results. This is confirmed on our bifurcation diagram for KCl, where the value of the steady calcium level is only slightly increasing for [KCl] > 30 mM (Fig. 7 *a*).

In vitro the mean calcium level (Lamboley et al., 2003) and the frequency (Zang et al., 2001; Mauban et al., 2001) decrease during maintained exposure to vasoconstrictors. Such effects, visible on Fig. 6, *e* and *f*, and on Fig. 8 *f*, are probably due to receptor and channel desensitization and photobleaching. They are not taken into account in our model.

CONCLUSION

The origin of arterial contraction and vasomotion is understood in terms of the calcium dynamics (flashing, recruitment, and synchronization) of a population of coupled SMCs. We have modeled the asynchronous flashing occurring at low vasoconstrictor concentration and explained why the number of recruited SMCs grows with increasing vasoconstrictor concentration. Moreover, we have shown that a weak gap junctional calcium coupling is necessary to synchronize calcium oscillations. Our results show that an electrical coupling can generate and desynchronize calcium oscillations. IP_3 diffusion does not play an important role in the achievement of synchronization. Our model is in agreement with the experimental results of Lamboley et al. (2003) obtained on strips of rat mesenteric arteries. We conclude that asynchronous flashing, recruitment, and synchronization, and thus arterial contraction and vasomotion, emerge from a population of coupled SMCs.

SUPPLEMENTARY MATERIAL

An online supplement to this article can be found by visiting BJ Online at http://www.biophysj.org.

This research was supported by Swiss National Science Foundation grant FN 31-61716.

REFERENCES

Achakri, H., A. Rachev, N. Stergiopoulos, and J. J. Meister. 1994. A theoretical investigation of low frequency diameter oscillations of muscular arteries. *Ann. Biomed. Eng.* 22:253–263.

Budel, S., A. Schuster, N. Stergiopoulos, J. J. Meister, and J. L. Beny. 2001. Role of smooth muscle cells on endothelial cell cytosolic free calcium in porcine coronary arteries. *Am. J. Physiol.* 281:H1156–H1162.

Christ, G. J., A. P. Moreno, A. Melman, and D. C. Spray. 1992. Gap junction-mediated intercellular diffusion of Ca^{2+} in cultured human corporal smooth muscle cells. *Am. J. Physiol.* 263:C373–C383.

Christ, G. J., D. C. Spray, M. el Sabban, L. K. Moore, and P. R. Brink. 1996. Gap junctions in vascular tissues. Evaluating the role of intercellular communication in the modulation of vasomotor tone. *Circ. Res.* 79:631–646.

Dora, K. A., M. P. Doyle, and B. R. Duling. 1997. Elevation of intracellular calcium in smooth muscle causes endothelial cell generation of NO in arterioles. *Proc. Natl. Acad. Sci. USA.* 94:6529–6534.

Dora, K. A., J. Xia, and B. R. Duling. 2003. Endothelial cell signaling during conducted vasomotor responses. *Am. J. Physiol.* 285:H119–H126.

Gonzalez-Fernandez, J. M., and B. Ermentrout. 1994. On the origin and dynamics of the vasomotion of small arteries. *Math. Biosci.* 119: 127–167.

Griffith, T. M., and D. H. Edwards. 1994. Fractal analysis of role of smooth muscle Ca^{2+} fluxes in genesis of chaotic arterial pressure oscillations. *Am. J. Physiol.* 266:H1801–H1811.

Haddock, R. E., G. D. Hirst, and C. E. Hill. 2002. Voltage independence of vasomotion in isolated irideal arterioles of the rat. *J. Physiol.* 540: 219–229.

Hamada, H., D. S. Damron, S. J. Hong, D. R. Van Wagoner, and P. A. Murray. 1997. Phenylephrine-induced Ca^{2+} oscillations in canine pulmonary artery smooth muscle cells. *Circ. Res.* 81:812–823.

Höfer, T. 1999. Model of intercellular calcium oscillations in hepatocytes: synchronization of heterogeneous cells. *Biophys. J.* 77:1244–1256.

Höfer, T., A. Politi, and R. Heinrich. 2001. Intercellular Ca^{2+} wave propagation through gap-junctional Ca^{2+} diffusion: a theoretical study. *Biophys. J.* 80:75–87.

Höfer, T., L. Venance, and C. Giaume. 2002. Control and plasticity of intercellular calcium waves in astrocytes: a modeling approach. *J. Neurosci.* 22:4850–4859.

LaBelle, E. F., and F. Polyak. 1996. Phospholipase C $\beta 2$ in vascular smooth muscle. *J. Cell. Physiol.* 169:358–363.

Lamboley, M., A. Schuster, J. L. Beny, and J. J. Meister. 2003. Recruitment of smooth muscle cells and arterial vasomotion. *Am. J. Physiol.* 285:H562–H569.

Li, X., and J. M. Simard. 1999. Multiple connexins form gap junction channels in rat basilar artery smooth muscle cells. *Circ. Res.* 84:1277–1284.

Lymn, J. S., and A. D. Hughes. 2000. Phospholipase C isoforms, cytoskeletal organization, and vascular smooth muscle differentiation. *News Physiol. Sci.* 15:41–45.

Mauban, J. R., C. Lamont, C. W. Balke, and W. G. Wier. 2001. Adrenergic stimulation of rat resistance arteries affects Ca^{2+} sparks, Ca^{2+} waves, and Ca^{2+} oscillations. *Am. J. Physiol.* 280:H2399–H2405.

Meininger, G. A., D. C. Zawieja, J. C. Falcone, M. A. Hill, and J. P. Davey. 1991. Calcium measurement in isolated arterioles during myogenic and agonist stimulation. *Am. J. Physiol.* 261:H950–H959.

Minneman, K. P. 1988. $\alpha 1$-adrenergic receptor subtypes, inositol phosphates, and sources of cell Ca^{2+}. *Pharmacol. Rev.* 40:87–119.

Moore, L. K., E. C. Beyer, and J. M. Burt. 1991. Characterization of gap junction channels in A7r5 vascular smooth muscle cells. *Am. J. Physiol.* 260:C975–C981.

Moore, L. K., and J. M. Burt. 1995. Gap junction function in vascular smooth muscle: influence of serotonin. *Am. J. Physiol.* 269:H1481–H1489.

Nelson, M. T., J. B. Patlak, J. F. Worley, and N. B. Standen. 1990. Calcium channels, potassium channels, and voltage dependence of arterial smooth muscle tone. *Am. J. Physiol.* 259:C3–C18.

Oishi, H., A. Schuster, M. Lamboley, N. Stergiopulos, J. J. Meister, and J. L. Beny. 2002. Role of membrane potential in vasomotion of isolated pressurized rat arteries. *Life Sci.* 71:2239–2248.

Parthimos, D., D. H. Edwards, and T. M. Griffith. 1999. Minimal model of arterial chaos generated by coupled intracellular and membrane Ca^{2+} oscillators. *Am. J. Physiol.* 277:H1119–H1144.

Peng, H., V. Matchkov, A. Ivarsen, C. Aalkjaer, and H. Nilsson. 2001. Hypothesis for the initiation of vasomotion. *Circ. Res.* 88:810–815.

Rebecchi, M. J., and S. N. Pentyala. 2000. Structure, function, and control of phosphoinositide-specific phospholipase C. *Physiol. Rev.* 80:1291–1335.

Ruehlmann, D. O., C. H. Lee, D. Poburko, and C. van Breemen. 2000. Asynchronous Ca^{2+} waves in intact venous smooth muscle. *Circ. Res.* 86:E72–E79.

Savineau, J. P., and R. Marthan. 2000. Cytosolic calcium oscillations in smooth muscle cells. *News Physiol. Sci.* 15:50–55.

Schuster, A., H. Oishi, J. L. Beny, N. Stergiopulos, and J. J. Meister. 2001. Simultaneous arterial calcium dynamics and diameter measurements: application to myoendothelial communication. *Am. J. Physiol.* 280: H1088–H1096.

Sell, M., W. Boldt, and F. Markwardt. 2002. Desynchronising effect of the endothelium on intracellular Ca^{2+} concentration dynamics in vascular smooth muscle cells of rat mesenteric arteries. *Cell Calcium.* 32: 105–120.

Shimamura, K., F. Sekiguchi, and S. Sunano. 1999. Tension oscillation in arteries and its abnormality in hypertensive animals. *Clin. Exp. Pharmacol. Physiol.* 26:275–284.

Sneyd, J., B. T. Wetton, A. C. Charles, and M. J. Sanderson. 1995. Intercellular calcium waves mediated by diffusion of inositol trisphosphate: a two-dimensional model. *Am. J. Physiol.* 268:C1537–C1545.

Ursino, M., G. Fabbri, and E. Belardinelli. 1992. A mathematical analysis of vasomotion in the peripheral vascular bed. *Cardioscience.* 3:13–25.

Verselis, V., R. L. White, D. C. Spray, and M. V. Bennett. 1986. Gap junctional conductance and permeability are linearly related. *Science.* 234:461–464.

Wagner, A. J., N. H. Holstein-Rathlou, and D. J. Marsh. 1996. Endothelial Ca^{2+} in afferent arterioles during myogenic activity. *Am. J. Physiol.* 270:F170–F178.

Wakui, M., B. V. Potter, and O. H. Petersen. 1989. Pulsatile intracellular calcium release does not depend on fluctuations in inositol trisphosphate concentration. *Nature.* 339:317–320.

Wang, S. S., A. A. Alousi, and S. H. Thompson. 1995. The lifetime of inositol 1,4,5-trisphosphate in single cells. *J. Gen. Physiol.* 105:149–171.

Wilkins, M., and J. Sneyd. 1998. Intercellular spiral waves of calcium. *J. Theor. Biol.* 191:299–308.

Yamamoto, Y., M. F. Klemm, F. R. Edwards, and H. Suzuki. 2001. Intercellular electrical communication among smooth muscle and endothelial cells in guinea-pig mesenteric arterioles. *J. Physiol.* 535: 181–195.

Yip, K. P., and D. J. Marsh. 1996. $[Ca^{2+}]_i$ in rat afferent arteriole during constriction measured with confocal fluorescence microscopy. *Am. J. Physiol.* 271:F1004–F1011.

Zang, W. J., C. W. Balke, and W. G. Wier. 2001. Graded $\alpha 1$-adrenoceptor activation of arteries involves recruitment of smooth muscle cells to produce ''all or none'' Ca^{2+} signals. *Cell Calcium.* 29:327–334.